Controllable Driven Phase Transitions in Fractional Quantum Hall States in Bilayer Graphene

Vadim M. Apalkov

Department of Physics and Astronomy, Georgia State University, Atlanta, Georgia 30303, USA

Tapash Chakraborty*

Department of Physics and Astronomy, University of Manitoba, Winnipeg, Canada R3T 2N2

(Received 24 February 2010; published 13 July 2010)

Here we report from our theoretical studies that, in biased bilayer graphene, one can induce phase transitions from an incompressible fractional quantum Hall state to a compressible state by tuning the band gap at a given electron density. The nature of such phase transitions is different for weak and strong interlayer coupling. Although for strong coupling more levels interact there is a lesser number of transitions than for the weak coupling case. The intriguing scenario of tunable phase transitions in the fractional quantum Hall states is unique to bilayer graphene and has never before existed in conventional semiconductor systems.

DOI: 10.1103/PhysRevLett.105.036801 PACS numbers: 73.43.Cd, 73.23.−b, 73.61.Wp

The unconventional quantum Hall effect in monolayer graphene, whose experimental observation [1] unleashed quite unprecedented interest in this system [2], reflects the unique behavior of massless Dirac fermions in a magnetic field [3,4]. In bilayer graphene this effect confirms the presence of massive chiral quasiparticles [5]. An important characteristic of bilayer graphene is that it is a semiconductor with a tunable band gap between the valence and conduction bands [6]. This modifies the Landau level spectrum and influences the role of long-range Coulomb interactions [7]. Here we report that the fractional quantum Hall effect (FQHE), a distinct signature of interacting electrons in the system [8,9], is very sensitive to the interlayer coupling strength and the bias voltage. We propose that by tuning the bias voltage one can induce phase transitions from an incompressible state to a compressible state at a given gate voltage. The bilayer graphene system shows quite different properties for weak and strong interlayer coupling. For a weak coupling the energy spectrum as a function of bias voltage shows a set of anticrossings, resulting in transitions from the FQHE state to a compressible state. At strong coupling there is a strong interaction between many energy levels, which finally results in only a few phase transitions. This interesting scenario of tunable phase transitions in the FQH states is unique to bilayer graphene. In conventional semiconductor systems, the type of phase transitions discussed below was never reported. The FQHE in monolayer graphene was in fact, studied theoretically by us [10] and subsequent experiments confirmed the existence of that effect in suspended monolayer graphene samples [11]. No such studies have been reported on bilayer graphene.

We assume that the bilayer graphene consists of two coupled graphene layers with the Bernal stacking arrangement. Our main concern then is the coupling between atoms of sublattice A of the lower layer and atoms of sublattice B' of the upper layer. The single-particle levels have twofold spin degeneracy and twofold valley degeneracy, which can be lifted in the many-particle systems at relatively large magnetic fields [12]. The valley degeneracy is also lifted under an applied bias voltage [5]. Considering only one spin direction, we describe the state of the system in terms of the four-component spinor $(\psi_A, \psi_B, \psi_{B'}, \psi_{A'})^T$ for valley K and $(\psi_{B'}, \psi_{A'}, \psi_A, \psi_B)^T$ for valley K'. Here subindices A, B and A', B' correspond to lower and upper layers, respectively. The strength of interlayer coupling is described in terms of the interlayer hopping integral, t. In a biased bilayer graphene the bias potential is introduced as the potential difference, ΔU, between the upper and lower layers. The Hamiltonian of the biased bilayer system in a perpendicular magnetic field then takes the form [5]

$$\mathcal{H} = \xi \begin{pmatrix} \Delta U/2 & v_F\pi_+ & \xi t & 0 \\ v_F\pi_- & \Delta U/2 & 0 & 0 \\ \xi t & 0 & -\Delta U/2 & v_F\pi_- \\ 0 & 0 & v_F\pi_+ & -\Delta U/2 \end{pmatrix}, \quad (1)$$

where $\pi_\pm = \pi_x \pm i\pi_y$, $\vec{\pi} = \vec{p} + e\vec{A}/c$, $\vec{p}$ is the two-dimensional electron momentum, $\vec{A}$ is the vector potential, $v_F \approx 10^6$ m/s is the Fermi velocity, and $\xi = +$ (K valley) or $-$ (K' valley).

In a perpendicular magnetic field the Hamiltonian (1) generates a discrete Landau level energy spectrum. The corresponding eigenfunctions can be expressed in terms of the conventional nonrelativistic Landau functions. The electron states in sublattices A and A' are written in terms of the nth Landau functions, while the electron states in sublattices B and B' are described by the $|n-1|$ and $n+1$ Landau functions, respectively. Therefore the Landau states in bilayer graphene can be described as a mixture of n, $n+1$, and $n-1$ nonrelativistic Landau functions belonging to different sublattices [6]. This mixture, for a given value of n, results in four different Landau levels. The Landau level energies, ε corresponding to the index n can be found from the following equation [6]

$$[(\varepsilon+\xi\delta)^2-2(n+1)][(\varepsilon-\xi\delta)^2-2n]=(\varepsilon^2-\delta^2)t^2, \quad (2)$$

where $\delta=\Delta U/2$ and all energies are expressed in units of $\hbar v_F/\ell_0$. Here $\ell_0=(\hbar/eB)^{1/2}$ is the magnetic length.

We now introduce a labeling scheme for Landau levels in bilayer graphene. From Eq. (2), we see that for each value of n ($=0, 1, 2, \ldots$) and in each valley there are four solutions, i.e., four Landau levels. Usually, the two lower Landau levels have negative energies and the two upper Landau levels have positive energies. Then each of the four Landau levels can be labeled as $n_i^{(\xi)}$, where $i=-2, -1, 1, 2$ is the label of the Landau level corresponding to the solution of Eq. (2) for a given value of n in the ascending order.

For a partially occupied Landau level the properties of the system, e.g., the ground state and excitations, are completely determined by the interelectron interactions, which can be expressed by Haldane's pseudopotentials, V_m, [13] (energies of two electrons with relative angular momentum m). In a graphene bilayer the Haldane pseudopotentials in a Landau level with index n and the energy ε have the form

$$V_m^{(n)}=\int_0^\infty \frac{dq}{2\pi} qV(q)[F_{n,\varepsilon}(q)]^2 L_m(q^2)e^{-q^2}, \quad (3)$$

where $L_m(x)$ are the Laguerre polynomials, $V(q)=2\pi e^2/(\kappa\ell_0 q)$ is the Coulomb interaction in the momentum space, κ is the dielectric constant, and $F_{n,\varepsilon}(q)$ are the corresponding form factors

$$F_{n,\varepsilon}(q)=\frac{1}{d_n}\Big[(1+f_n^2)L_n(\tfrac{q^2}{2})+\frac{2n}{(\varepsilon-\xi\delta)^2}L_{n-1}(\tfrac{q^2}{2}) + \frac{2(n+1)}{(\varepsilon+\xi\delta)^2}f_n^2 L_{n+1}(\tfrac{q^2}{2})\Big], \quad (4)$$

where $f_n=\frac{(\varepsilon-\xi\delta)^2-2n}{t(\varepsilon-\xi\delta)}$ and $d_n=1+f_n^2+\frac{2n}{(\varepsilon-\xi\delta)^2}+\frac{2(n+1)}{(\varepsilon+\xi\delta)^2}f_n^2$.

The form factors of bilayer graphene [Eq. (4)] are clearly different from the corresponding ones for a monolayer graphene. In the latter case, the form factor of the $n=0$ Landau level is the same as that of conventional nonrelativistic electrons [10,14], $F_0(q)=L_0$. The form factors of higher Landau levels are determined by the mixture of L_n and L_{n+1} terms. In bilayer graphene the form factors of the $n=0$ Landau level are mixtures of the L_0 and L_1 terms and are different from that in the nonrelativistic case. There is one special Landau level in bilayer graphene with index $n=0$, whose properties are completely identical to that of the nonrelativistic $n=0$ Landau level. It is clear from Eq. (2) that for $n=0$ there is a Landau level with energy $\epsilon=\xi\delta$. This energy does not depend on the coupling between the layers, t. The form factor of this Landau level is exactly equal to the form factor of a nonrelativistic system of the $n=0$ Landau level, $F_{n=0,\epsilon=\xi\delta}=L_0$. Therefore, all many-body properties of a bilayer system in the $n=0$, $\epsilon=\xi\delta$ Landau level are completely identical to those of a nonrelativistic conventional system in the $n=0$ Landau level.

For Landau levels with higher indices, the form factor is a mixture of three different functions, L_n, L_{n-1}, and L_{n+1}. Therefore, in general, the strength of interelectron interactions in bilayer graphene is strongly modified as compared to its value in monolayer graphene. To address the effects of these modifications on the properties of the many-electron system in bilayer graphene we investigate fractional filling factors corresponding to the FQHE [8]. We treat the many-electron system at various fractional filling factors numerically within the spherical geometry [10,13]. The radius of our sphere is $R=\sqrt{S}\ell_0$, where $2S$ is the number of magnetic fluxes through the sphere in units of the flux quanta. The single-electron states are characterized by the angular momentum, S, and its z component, S_z. For the many-electron system the corresponding states are classified by the total angular momentum L and its z component, while the energy of the state depends only on L [15]. A given fractional filling of the Landau level is determined by a special relation between the number of electrons N and the radius of the sphere R. For example, the $\frac{1}{3}$-FQHE state is realized at $S=(\frac{3}{2})(N-1)$, while the $\frac{2}{5}$-FQHE state corresponds to the relation $S=(\frac{5}{4})N-2$. With the Haldane pseudopotentials [Eq. (3)], we determine the interaction Hamiltonian matrix [15] and then calculate a few lowest eigenvalues and eigenvectors of this matrix. The FQHE states are obtained when the ground state of the system is an incompressible liquid, the energy spectrum of which has a finite many-body gap [8,9].

We begin with the celebrated $\frac{1}{3}$-FQHE [9], corresponding to the filling factor $\nu=\frac{1}{3}$. The behavior of the Landau level spectra as a function of the bias voltage and for different values of t are displayed in Fig. 1 (only the Landau levels with positive energies are shown). A similar behavior is valid for other FQHE filling factors, e.g., for $\nu=\frac{2}{5}$ [16]. Figure 1 clearly illustrates that the FQHE can be observed in all $n=0$ Landau levels with the strongest FQHE being in the second $n=0$ Landau levels of both valleys, i.e., $0_2^{(+)}$ and $0_2^{(-)}$.

We found an interesting behavior in the $n=1$ Landau levels. There are four such levels with positive energy, two per valley. The FQHE in these levels shows different properties depending on the strength of t. For all parameters of the system there is no FQHE in the Landau level $1_2^{(-)}$. At small values of t, $t\lesssim 150$ meV, [Fig. 1(a)] the system clearly shows few *anticrossings* accompanied by the transitions from the FQHE incompressible state to a state without the FQHE. There is one such transition for levels $1_2^{(+)}$ and $1_1^{(-)}$, but there are two transitions in level $1_1^{(+)}$, corresponding to two anticrossings in this level. Thus, in level $1_1^{(+)}$ and small ΔU, the FQHE is present but disappears at larger values of ΔU. It reappears at very large values of $\Delta U(\approx 400$ meV). With increasing t the

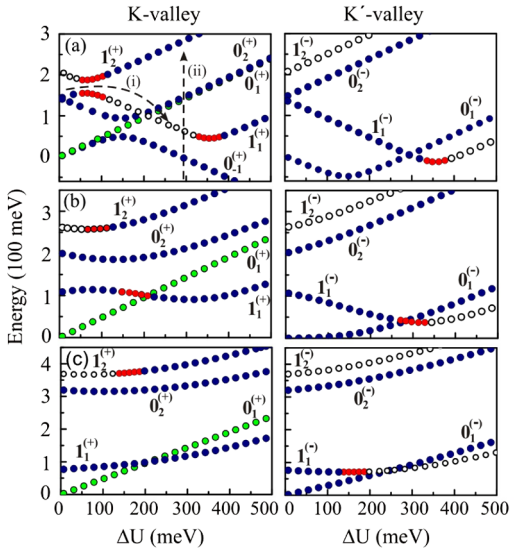

FIG. 1 (color online). A few lowest Landau levels of the conduction band (for two valleys) as a function of the bias potential, ΔU, for different values of interlayer coupling: (a) $t = 30$ meV, (b) $t = 150$ meV, and (c) $t = 300$ meV, and a magnetic field of 15 Tesla. The numbers next to the curves denote the corresponding Landau levels. The Landau levels where the $\frac{1}{3}$-FQHE can be observed are drawn as blue (dark gray) and green (light gray) filled dots. The green (light gray) dots correspond to the Landau levels where the FQHE states are identical to that of a monolayer of graphene. The red (medium gray) dots represent Landau levels with weak $\frac{1}{3}$-FQHE and the open dots for those where the FQHE is absent. In (a), the dashed lines labeled by (i) and (ii) illustrate two situations: (i) under a constant gate voltage and variable bias potential; (ii) under a constant bias potential and variable gate voltage.

two anticrossings in level $1_1^{(+)}$ merge [see Fig. 1(b)] and finally disappear [Fig. 1(c)]. At large values of t, $t >$ 150 meV, there are only two anticrossings [Fig. 1(c)] in $1_1^{(-)}$ and $1_2^{(+)}$ Landau levels. At such large values of t, the anticrossings cannot be considered as an interaction between two "crossing" levels, but as a result of strong interaction between all (four) levels of the two layers of bilayer graphene. It is important that such strong interaction between the levels does not destroy the FQHE, but shows well-defined regions with strong FQHE. For weak coupling between graphene monolayers, i.e., for a small t, transitions from the $\frac{1}{3}$-FQHE state to a non-FQHE state can be understood in terms of the anticrossing of $n = 1$ and $n = 2$ Landau levels of the monolayers. For monolayers, the FQHE can be observed only in the $n = 0$ and 1 Landau levels but not for $n = 2$ [10]. The levels without the FQHE in Fig. 1(c) then correspond to $n = 2$ of one of the monolayers. For large t, i.e., for strong coupling, such a simple description is however inadequate. The properties of the $n = 1$ levels have important implications for possible experimental observations of this unique behavior [Fig. 1(a)].

(i) By applying a gate voltage the electron density can be tuned so that the first four Landau levels are completely occupied and the next Landau level is partially occupied with the FQHE filling factor, for example, $\nu = \frac{1}{3}$. Following Fig. 1(a), this means that the $0_{-1}^{(+)}$, $0_1^{(+)}$, $1_1^{(-)}$, $0_2^{(+)}$ Landau levels are fully occupied, while the $1_1^{(+)}$ Landau level has a filling factor $\frac{1}{3}$. Then, by varying ΔU from a small value, e.g., 10 meV, to a larger value, e.g., 200 meV, one can observe the disappearance of the FQHE [line (i) in Fig. 1(a)].

(ii) The bias voltage is kept fixed at a large value, e.g., $\Delta U = 300$ meV. Then by varying the gate voltage and thus increasing the electron density, one can observe the disappearance and reappearance of the 1/3-FQHE in higher Landau levels [line (ii) in Fig. 1(a)], when the filling factors of the corresponding Landau levels are 1/3.

The collapse of the FQHE gap corresponding to the appearance of anticrossing of the $n = 1$ Landau levels, is illustrated in Fig. 2. The FQHE gap has a monotonic dependence on the bias voltage. In the anticrossing region the gap disappears for the lower $n = 1$ Landau level [Fig. 2(a)] and reappears for the higher $n = 1$ Landau level [Fig. 2(b)]. The evolution of the energy spectra of the incompressible liquid is found to be similar for other filling factors (such as $\nu = \frac{2}{5}$ [16]). This behavior was never before observed in the FQHE of conventional two-dimensional electron systems.

The strength of the FQHE, i.e., the magnitude of the excitation gap, depends on the bias voltage and the interlayer hopping integral. In Fig. 3, this dependence is shown for $\frac{1}{3}$-FQHE in different Landau levels as a function of t. In accordance with the properties of Haldane pseudopotentials, the excitation gap of the $0_1^{(+)}$ Landau levels does not depend on the bias voltage and on the interlayer hopping integral. The corresponding gap remains constant and is equal to the gap of the FQHE in a single layer of graphene in the $n = 0$ Landau level. For $t = 0$ the two layers of graphene are decoupled and the bilayer system becomes identical to a monolayer with additional double degeneracy. This property is clearly seen in Fig. 3, where for $t = 0$ there are only two doubly degenerate FQHE gaps,

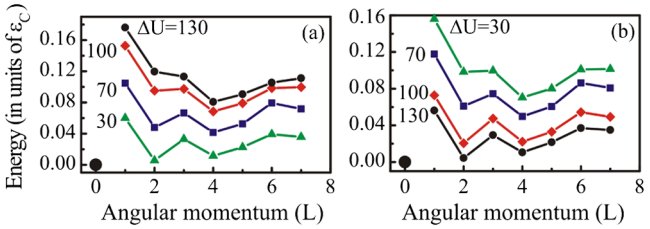

FIG. 2 (color online). Low-energy excitation spectra of the $\frac{1}{3}$-FQHE states (eight electrons) in the Landau levels (a) $1_{(2)}^{(+)}$, and (b) $1_{(1)}^{(+)}$, shown for different values of the bias potential (the numbers next to the lines are the values of ΔU in meV). The system is fully spin polarized. The interlayer hopping integral is set to 30 meV and the magnetic field is 15 Tesla. The flux quanta is $2S = 21$. The solid dot at $L = 0$ depicts the ground state. The energy unit is $\varepsilon_c = e^2/\kappa\ell_0$.

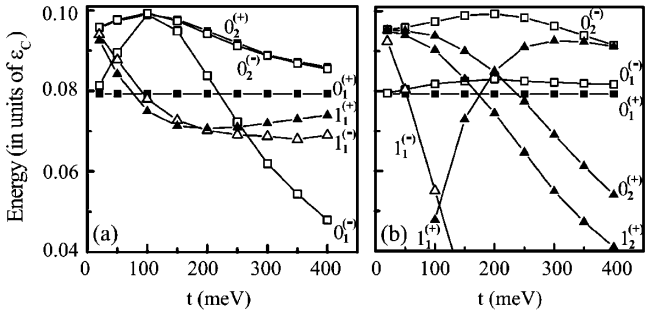

FIG. 3. The FQHE gaps are shown for different Landau levels. The labels next to the lines correspond to the labeling of Landau levels shown in Fig. 1. $\nu = \frac{1}{3}$-FQHE (eight electron) for (a) $\Delta U = 10$ meV, and (b) $\Delta U = 300$ meV. All systems are fully spin polarized.

corresponding to $n = 0$ and $n = 1$ single layer Landau levels.

At the zero bias voltage the system has twofold valley degeneracy, which is lifted at finite values of ΔU. At a small bias voltage, $\Delta U = 10$ meV, the levels belonging to two valleys are almost degenerate, which results in almost the same FQHE gaps of the corresponding levels. At the same time the FQHE gaps of $0_1^{(+)}$ and $0_1^{(-)}$ levels, which are degenerate at the zero bias voltage, are different. The origin of these levels is the following: At the zero bias voltage there is a fourfold degenerate Landau level with zero energy ($0_1^{(+)}$, $0_1^{(-)}$, $0_{-1}^{(+)}$, and $0_{-1}^{(-)}$). At a finite bias voltage, two of the levels have positive energies (shown in Fig. 1) and the other two levels have negative energies. At small values of ΔU, the wave functions corresponding to the levels $0_1^{(+)}$ and $0_{-1}^{(+)}$ of valley K have the form $(0, 0, 0, \phi_0)$ and $(\phi_0, 0, 0, (t/2^{1/2})\phi_1)$, respectively. Here ϕ_n are nth "nonrelativistic" Landau functions and t is in units of $\hbar v_F/\ell_0$. The corresponding form factors $F(q)$, are L_0 for level $0_1^{(+)}$ and $\frac{L_0+(t^2/2)L_1}{1+t^2/2}$ for level $0_1^{(-)}$. Although the energies of these levels are almost the same the form factors and hence the gaps are quite different. In Fig. 3(a) this difference is clearly visible. The dependence of the gap of the FQHE of level $0_1^{(-)}$ on parameter t is nonmonotonic. At $t = 0$ the form factor of level $0_1^{(-)}$ is L_0 and the FQHE gap is exactly equal to the FQHE gap in the $n = 0$ Landau level of a single graphene layer. At $t = 2^{1/2}\hbar v_F/\ell_0$ the form factor is $\frac{L_0+L_1}{2}$ and the FQHE gap is equal to that in the $n = 1$ Landau level of a single graphene layer. This point corresponds to the maximum in Fig. 3(a). At a large bias voltage, $\Delta U = 300$ meV [Fig. 3(b)], the FQHE gaps show mainly monotonic dependence on the hopping integral. The FQHE gaps of the levels $0_1^{(+)}$ and $0_1^{(-)}$, which were quite different in Fig. 3(a), are now close. There is also disappearance of the FQHE in some $n = 1$ Landau levels, which corresponds to the anticrossing behavior in Fig. 1. Similar results are also found for the filling factor $\nu = \frac{2}{5}$ (i.e., FQHE ↔ non-FQHE transitions occur at the same Landau levels and at similar values of ΔU) [16].

To summarize, we have clearly demonstrated that bilayer graphene in a strong perpendicular magnetic field reveals some unique properties, which could allow novel transitions from the FQHE state to a vanishing FQHE state. These transitions occur within the same Landau level by varying the bias voltage, i.e, the potential difference between the layers. Similarly, we have shown that our work on bilayer graphene also results in new physics: The transitions FQHE ↔ zero-FQHE, which for weak interlayer coupling can be explained as the result of anticrossing of two levels, also persists in the limit of strong coupling, where all levels are strongly coupled. We have established here that there is a fundamental difference between the two regimes of weak and strong coupling in bilayer graphene. The boundary between the two regions is determined by the dimensionless parameter $[t/(\hbar v_F/\ell_0)] \sim 1.5$.

We wish to thank David Abergel and Julia Berashevich for very helpful discussions. The work has been supported by the Canada Research Chairs Program.

*tapash@physics.umanitoba.ca

[1] K. S. Novoselov *et al.*, Nature (London) **438**, 197 (2005); Y. Zhang *et al.*, *ibid.* **438**, 201 (2005).
[2] D. S. L. Abergel, V. Apalkov, J. Berashevich, K. Ziegler, and T. Chakraborty, Adv. Phys. (to be published).
[3] P. R. Wallace, Phys. Rev. **71**, 622 (1947).
[4] J. W. McClure, Phys. Rev. **104**, 666 (1956).
[5] K. S. Novoselov *et al.*, Nature Phys. **2**, 177 (2006); E. McCann and V. Falko, Phys. Rev. Lett. **96**, 086805 (2006); E. McCann, Phys. Rev. B **74**, 161403 (2006); T. Ohta *et al.*, Science **313**, 951 (2006); E. V. Castro *et al.*, Phys. Rev. Lett. **99**, 216802 (2007); M. Koshino and E. McCann, Phys. Rev. B **81**, 115315 (2010).
[6] J. M. Pereira, Jr., F. M. Peeters, and P. Vasilopoulos, Phys. Rev. B **76**, 115419 (2007).
[7] D. S. L. Abergel and T. Chakraborty, Phys. Rev. Lett. **102**, 056807 (2009).
[8] T. Chakraborty, and P. Pietiläinen, *The Quantum Hall Effects* (Springer, New York, 1995), 2nd ed; T. Chakraborty, Adv. Phys. **49**, 959 (2000).
[9] D. C. Tsui, H. L. Störmer, and A. C. Gossard, Phys. Rev. Lett. **48**, 1559 (1982); R. B. Laughlin, *ibid.* **50**, 1395 (1983).
[10] V. M. Apalkov and T. Chakraborty, Phys. Rev. Lett. **97**, 126801 (2006).
[11] K. I. Bolotin *et al.*, Nature (London) **462**, 196 (2009); see also, X. Du *et al.*, *ibid.* **462**, 192 (2009).
[12] M. Nakamura, E. V. Castro, and B. Dora, Phys. Rev. Lett. **103**, 266804 (2009); Y. Zhao *et al.*, *ibid.* **104**, 066801 (2010).
[13] F. D. M. Haldane, Phys. Rev. Lett. **51**, 605 (1983).
[14] M. O. Goerbig, R. Moessner, and B. Doucot, Phys. Rev. B **74**, 161407(R) (2006).
[15] G. Fano, F. Ortolani, and E. Colombo, Phys. Rev. B **34**, 2670 (1986).
[16] V. Apalkov and T. Chakraborty (unpublished).